JOURNAL OF COLLOID AND INTERFACE SCIENCE **176,** 397–407 (1995)

Electrostatic Interactions between a Charged Sphere and a Charged Planar Surface in an Electrolyte Solution

JAN STÅHLBERG,*[,1] ULF APPELGREN,† AND BENGT JÖNSSON‡

*Department of Analytical Chemistry, University of Stockholm, S-106 91 Stockholm, Sweden; †Department of Quality Control, Astra Production Chemicals AB, S-151 85 Södertälje, Sweden; and ‡Division of Physical Chemistry 1, Chemical Center, University of Lund, S-221 00 Lund, Sweden

Received January 26, 1995; accepted May 2, 1995

The electrostatic interaction energy for a charged sphere interacting with a low dielectric charged planar surface in an electrolyte solution is calculated. The calculations are based on a solution of the linearized Poisson–Boltzmann equation under the condition of constant charge density on both surfaces. The influence of sphere size, its dielectric constant, and net charge as well as planar surface charge density and electrolyte concentration on the interaction energy is demonstrated. A comparison is made between the interaction energies for a point charge interacting with a charged planar surface, calculated from the Gouy–Chapman theory, and our solution for a charged 2.5 Å sphere. The calculations show an asymmetric interaction energy for spheres of opposite sign of charge, i.e., when the surface and sphere are of the same (opposite) sign the interaction is stronger (weaker) than what is obtained from the Gouy–Chapman theory. On the other hand, the asymmetry is overestimated when the Deryaguin procedure is applied to calculate the interaction energy between a charged sphere and a charged planar surface. In the latter case the asymmetry is mainly due to overestimation of the repulsive energy when the sphere and the planar surface have the same sign of charge. It is shown that, as a first approximation, the interaction energy can be obtained by adding the contribution from three separate components: a point charge, located in the center of the sphere, interacting with the charged surface plus the interaction energy between an uncharged sphere and the charged surface plus the interaction energy between a charged sphere and the uncharged surface.

Key Words: electrostatic interaction; charged sphere–planar surface; linearized Poisson–Boltzmann equation; adsorption; proteins.

INTRODUCTION

The electrostatic interaction between a charged sphere and a charged planar low dielectric surface in an electrolyte solution is, from a physicochemical point of view, a complex problem. The reason for this is that it must account for the ''three body'' interaction between the surface–sphere–electrolyte which all simultaneously influence each other. The system is however of wide practical and theoretical interest where important examples are the interaction between a surface and micelles, charged polymers, or charged colloid particles, respectively. Our interest for this system stems from the view that electrostatic interaction is of great importance in the description and understanding of protein adsorption. The reason is that many proteins are globular and charged and it is reasonable to assume that they can be approximated as charged spheres. In an earlier paper (1) we showed that retention changes of proteins in ion exchange chromatography, due to changes in electrolyte concentration in the mobile phase, could be described by using a model based on the electrostatic interaction between two oppositely charged planar surfaces. The charged sphere–planar surface system may therefore be a complement to this model in the description of electrostatic interactions in protein adsorption studies.

Even though advances have been made in the molecule dynamic and Monte Carlo calculations of electrostatic interactions in surface and colloid chemistry, solutions of the Poisson–Boltzmann (P–B) equation are also useful tools for the calculation of these interactions. Although the limitations of Poisson–Boltzmann approach are well known, i.e., the mean field approximation and the assumption of point charges, many studies have shown that it agrees surprisingly well with more sophisticated computer simulations as well as with experimental results. Generally speaking, deviations from the P–B result occur at high ionic strengths, high surface charge densities, or when higher charged small ions are present in the electrolyte solution. However, a closed form analytical solution to the P–B equation is only available for a limited number of cases. For low surface potentials the exponential terms in the P–B equation can be linearized and the resulting linear second-order differential equation has been solved analytically for a charged sphere (2) and a charged cylinder (3) in an electrolyte solution. For the interaction between two charged bodies a closed-form analytical solution is available for two planar surfaces interacting in an electrolyte. By applying the Dery-

[1] To whom correspondence should be addressed.

0021-9797/95 $12.00

aguin procedure the repulsive electrostatic interaction between charged spherical particles of identical radius under conditions of identical and constant potential constitutes the electrostatic contribution in the well known DLVO theory (4, 5). Using statistical mechanical equilibrium theories for liquids Medina-Noyola and McQuarrie showed that the equations obtained by Verwey and Overbeek are valid for all separation distances between the particles (6). Hogg *et al.* (7) later applied the Deryaguin procedure for developing expressions for potential energies of unequal charged spheres of low surface potentials. Many papers have since then suggested improvements of the Deryaguin procedure (8–13).

The interaction between a charged sphere and a charged planar surface in an electrolyte solution has previously been discussed in two Russian papers by Kaplan *et al.* (14, 15) for the constant potential case. More recently Carnie *et al.* used the linearized Poisson–Boltzmann equation to calculate the interaction free energy between charged spheres of unequal sizes (16). An exact solution of the linearized Poisson–Boltzmann equation for the electrostatic interaction between a charged ion-penetrable sphere and a charged plate has been given by Ohshima and Kondo (17).

The traditional approach to calculate the interaction between a charged sphere and a planar surface in an electrolyte solution would either be to neglect the influence of the size of the sphere and approximate the interaction as between a point charge and the surface or to use the Deryaguin procedure neglecting *inter alia* the dielectric properties of the sphere. In this paper a solution of the linearized P–B equation is developed for this system including the dielectric properties of the charged sphere and under the condition of constant surface charge density on the two bodies. It is shown how the size and dielectric constant of the sphere influences the electrostatic interaction and that the neglect of these parameters in many cases gives erronous results.

THEORY

A schematic representation of the model system used in the calculations is found in Fig. 1. The center of a spherical aggregate with radius a is placed a distance Z_0 from the planar interface of a macroscopic low dielectric region. The dielectric property of the three regions, electrolyte solution, spherical aggregate, and the macroscopic low dielectric region, is described by the three dielectric constants ε_w, ε_s, and ε_p. The Laplace equation (18), Eq. [1], is used to determine the electrostatic potential, Φ, in the interior of the spherical aggregate and in the macroscopic low dielectric region:

$$\nabla^2\Phi = 0. \qquad [1]$$

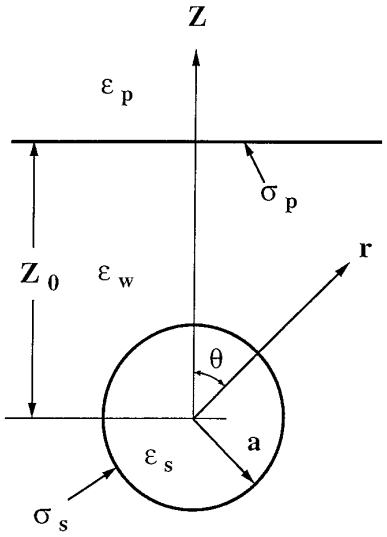

FIG. 1. Description of the geometrical and physical parameters for the sphere–planar surface system.

The electrostatic properties of the electrolyte solution are described by the linearized Poisson–Boltzmann equation (17)

$$\nabla^2\Phi = \kappa^2\,\Phi, \qquad [2]$$

where ∇^2 is the Laplace operator and κ is the inverse Debye length of the electrolyte solution. The electrostatic potential in the electrolyte solution, region $r > a$ and $Z < Z_0$ in Fig. 1, can be written as the sum of three contributions:

1. The potential from the surface charges on the planar interface, Φ_p.
2. The potential from the surface charges and induced surface charges on the spherical aggregate, Φ_s.
3. The potential from the induced surface charges on the planar interface, Φ_{image}.

Each of these contributions will now be discussed and equations for their dependence on different parameters will be derived.

The electrostatic potential from the surface charges on the planar interface, Φ_p, is easy to calculate from the linearized Poisson–Boltzmann equation when a Cartesian coordinate system (X, Y, Z) is used. The equation for the distance dependence of the potential becomes (19):

$$\Phi_p(X, Y, Z) = \Phi_0 \times e^{\kappa(Z - Z_0)}, \qquad [3]$$

where Φ_0 is the surface potential of the undisturbed interface. This equation can also be written as a function of the two coordinates (r, θ) in a spherical coordinate system centered in the sphere; see Fig. 1. Using the modified spherical Bessel functions of the first kind $i_n(\kappa r)$ and the Legendre polynomi-

als $P_n(\cos\theta)$, the equation for the potential from the surface charges on the planar interface can be written as (20, 21)

$$\begin{aligned}\Phi_p(r,\theta) &= \Phi_0 \times e^{-\kappa Z_0} \times \sum_{n=0}^{\infty} (2n+1)\, i_n(\kappa r)\, P_n(\cos\theta). \quad [4]\end{aligned}$$

The surface charges and induced surface charges on the spherical aggregate give rise to an electrostatic potential Φ_s which can be written as the sum of the potentials from a multipole expansion, C_n, of the charge distribution (18). The magnitude of each of these multipole moments is later in the calculations determined from the boundary conditions at the two interfaces at $Z = Z_0$ and $r = a$. By using the multipole expansion, the electrostatic potential in the electrolyte solution from the charged spherical aggregate becomes (18, 20)

$$\Phi_s(r,\theta) = \sum_{n=0}^{\infty} C_n \times k_n(\kappa r) \times P_n(\cos\theta), \quad [5]$$

where C_n is the nth multipole moment of the sphere and $k_n(\kappa r)$ is a modified spherical Bessel function of the third kind of order n.

The electrostatic potential from the sphere, Φ_s, induces surface charges on the interface $Z = Z_0$. These induced surface charges will also give a contribution to the electrostatic potential in the electrolyte solution, Φ_{image}. The connection between Φ_{image} and Φ_s can easily be obtained from the boundary conditions at $Z = Z_0$ if a cylindrical coordinate system with the symmetry axis along the Z-axis in Fig. 1 is used. The equations for the different potentials can in this coordinate system be written as (22)

$$\begin{aligned}\Phi(r,z) &= \int_0^{\infty} FA(k)\, e^{-\sqrt{k^2+\kappa^2}\, Z} J_0(kr)\, dk \\ &+ \int_0^{\infty} FB(k)\, e^{\sqrt{k^2+\kappa^2}\, Z} J_0(kr)\, dk \quad 0 < Z < Z_0 \quad [6a]\end{aligned}$$

and

$$\Phi(r,z) = \int_0^{\infty} FC(k)\, e^{-kZ} J_0(kr)\, dk \quad Z > Z_0, \quad [6b]$$

where $J_0(kr)$ is a Bessel function of order n and $FA(k)$, $FB(k)$, and $FC(k)$ are k-dependent functions. The first integral in Eq. [6a] gives Φ_s and the second integral gives Φ_{image}. The connection between $FA(k)$ and $FB(k)$ are determined from the boundary conditions that the potential and the dielectric displacement is continuous at $Z = Z_0$. The following relation is obtained:

$$\begin{aligned}FB(k) &= \frac{\epsilon_w\sqrt{k^2+\kappa^2} - \epsilon_p k}{\epsilon_w\sqrt{k^2+\kappa^2} + \epsilon_p k} \times FA(k)\, e^{-2\sqrt{k^2+\kappa^2}\, Z_0} \\ &\approx FA(k)\, e^{-2\sqrt{k^2+\kappa^2}\, Z_0} \quad \text{if } \epsilon_w \gg \epsilon_p. \quad [7]\end{aligned}$$

This means that the effect of the low dielectric salt free region, i.e., $Z > Z_0$, on the potential in the electrolyte solution, $Z < Z_0$, can, as long as $\epsilon_w \gg \epsilon_p$, be approximated by a system where the electrolyte solution is extended to the region $Z > Z_0$ and an image multipole is placed at $Z = 2Z_0$. The magnitude of each image multipole moment is equal to the corresponding multipole moment for the sphere:

$$C_n(\text{image}) = C_n. \quad [8]$$

The relative error in Φ_{image} arising from this approximation is always less than $2\epsilon_p/(\epsilon_w + \epsilon_p)$ and, in most cases, much less then this value.

The equation for the electrostatic potential from the image multipole has the same form as Eq. [5] when a coordinate system centered at $Z = 2Z_0$ is used:

$$\Phi_{image}(r_i,\theta_i) = \sum_{n=0}^{\infty} C_n \times k_n(\kappa r_i) \times P_n(\cos\theta_i). \quad [9]$$

Here r_i is the distance from the center of the image multipole and θ_i is the angle between the vector $\mathbf{r}_i$ and a vector from $Z = 2Z_0$ to $Z = 0$. The image potential can also be written as a function of the coordinates r and θ (see Fig. 1),

$$\begin{aligned}\Phi_{image}(r,\theta) &= \sum_{n=0}^{\infty}\sum_{m=0}^{\infty} C_m \times A_{n,m} \times i_n(\kappa r) \\ &\times P_n(\cos\theta) \quad \text{if } a < r < 2Z_0 - a, \quad [10]\end{aligned}$$

where the coefficients $A_{n,m}$ are obtained by comparing Eqs. [9] and [10]. When this comparison is made along the Z-axis, an equation which always must be fulfilled for the $A_{n,m}$ coefficients is obtained:

$$k_m(\kappa \times (2Z_0 - Z)) = \sum_{m=0}^{\infty} A_{n,m} \times i_m(\kappa Z). \quad [11]$$

By use of the addition theorem and the recurrence relations for Bessel functions (20, 21) the equations for the $A_{n,m}$ coefficients become

$$A_{n,0} = A_{0,n} = (2n+1) \times k_n(\kappa \times 2Z_0) \quad [12a]$$

$$A_{n,1} = A_{1,n} = -(2n+1) \times k_n'(\kappa \times 2Z_0) \quad [12b]$$

$$A_{n,m+1} = -\frac{m}{m+1} A_{n,m-1} + \frac{2m+1}{m+1} \times \frac{n+1}{2n+3} A_{n+1,m} + \frac{2m+1}{m+1} \times \frac{n}{2n-1} A_{n-1,m}. \quad [12c]$$

By summing the three contributions to the electrostatic potential in the electrolyte solution, Eqs. [4], [5], and [10], the following equation is obtained:

$$\emptyset(r,\theta) = \sum_{n=0}^{\infty} \{\emptyset_0 e^{-\kappa Z_0} (2n+1) i_n(\kappa r) + C_n k_n(\kappa r) + \sum_{m=0}^{\infty} C_m A_{n,m} i_n(\kappa r)\} \times P_n(\cos\theta). \quad [13]$$

The distance and angle dependence of the electrostatic potential in the charge free interior of the spherical aggregate can be expressed by use of the Laplace equation as (18)

$$\emptyset(r,\theta) = \sum_{n=0}^{\infty} B_n \times r^n \times P_n(\cos\theta). \quad [14]$$

The two potentials, Eqs. [13] and [14], shall satisfy two boundary conditions at the interface $r = a$,

$$\emptyset(a-) = \emptyset(a+) \quad [15a]$$

and

$$\epsilon_w \frac{d\emptyset(a+)}{dr} - \epsilon_s \frac{d\emptyset(a-)}{dr} = -\frac{\sigma_s}{\epsilon_0} = -\sum_{n=0}^{\infty} \frac{\sigma_{s,n}}{\epsilon_0} \times P_n(\cos\theta), \quad [15b]$$

where σ_s is the charge density of the sphere and ϵ_0 is the permittivity in vacuum (the polarization-charge density of the sphere is not included in σ_s). In the second part of Eq. [15b] the surface charge density has been expanded in the multipole expansion $\Sigma\, \sigma_{s,n} P_n(\cos\theta)$.

At the interface $r = a$, and for each n value, the two potential equations, Eqs. [13] and [14], are equal giving

$$\sum_{m=0}^{\infty} A_{n,m} C_m + K_n C_n = -S_n - (2n+1) \emptyset_0 e^{-\kappa Z_0}, \quad [16a]$$

where the coefficients K_n and S_n are

$$K_n = \frac{\epsilon_w \kappa a\, k_n'(\kappa a) - \epsilon_s n\, k_n(\kappa a)}{\epsilon_w \kappa a\, i_n'(\kappa a) - \epsilon_s n\, i_n(\kappa a)} \quad [16b]$$

$$S_n = \frac{\sigma_{s,n} \times a}{\epsilon_0(\epsilon_w \kappa a\, i_n'(\kappa a) - \epsilon_s n\, i_n(\kappa a))}. \quad [16c]$$

When the sum over m in Eq. [16a] is truncated at $m = N$ and for each choosen n value there will be $N + 1$ unknown multipole moments $(C_0, C_1, \ldots, C_N)$. These C_n values can, however, be calculated from a set of equations consisting of the first $N + 1$ different n values in Eq. [16a].

The effective interaction between the charged sphere and the low dielectric region and the surface charges on the planar interface can be calculated by using the obtained equation for the electrostatic potential in the electrolyte solution. This calculation can be done by several different methods and we have used a charged integration where the energy needed to charge the interface and sphere from zero to full charge is calculated.

The following equation for the interaction between the sphere and the planar surface is obtained:

$$G_{el} = \frac{\sigma_p}{2} \times \int_{interface} \emptyset_s(Z_0) + \emptyset_{image}(Z_0)\, dA + \frac{1}{2} \times \int_{sphere} \sigma_s \times \Delta\emptyset(a)\, dA. \quad [17]$$

Here $\Delta\emptyset(a)$ is the difference in the electrostatic potential on the sphere surface when the distance between the sphere and the interface changes from ∞ to Z_0. The surface potential of the undisturbed interface, $\emptyset_0$, can be obtained from the surface charge density of the planar interface, σ_p, by use of Gauss' law (18)

$$\emptyset_0 = \frac{\sigma_p}{\epsilon_0 \epsilon_w \kappa}. \quad [18]$$

By using Eqs. [5], [10], and [13] for $\emptyset_s(Z_0)$, $\emptyset_{image}(Z_0)$, and $\emptyset(a)$, respectively, the two integrals in Eq. [17] can be solved. After a lot of algebraic manipulations the final result becomes

$$\frac{\sigma_p}{2} \times \int_{interface} \emptyset_s(Z_0) + \emptyset_{image}(Z_0)\, dA = \frac{2\pi\, \sigma_p}{\kappa^2} \times e^{-\kappa Z_0} \times \sum_{n=0}^{\infty} C_n \quad [19a]$$

and

$$\frac{1}{2} \int_{sphere} \sigma_s \Delta\emptyset(a)\, dA = 2\pi a^2 \sum_{n=0}^{\infty} \sigma_{s,n} \left\{ \emptyset_0 e^{-\kappa Z_0} i_n(\kappa a) + \frac{\Delta C_n k_n(\kappa a)}{2n+1} + \frac{i_n(\kappa a)}{2n+1} \sum_{m=0}^{\infty} C_m A_{n,m} \right\}, \quad [19b]$$

where ΔC_n is the difference in C_n value when the distance between the sphere and the interface is Z_0 and ∞, respectively.

The number of multipole moments, N, needed for convergence in the calculations depends on the size of the sphere and the distance between the sphere and the planar interface. An N value of about 10 was enough for the examples presented in this work; i.e., the potentials and energies obtained for N values 10, 20, and 40 were equal to within 1%.

RESULTS AND DISCUSSION

In a moderately concentrated electrolyte solution (ionic strength < 0.1 mol/liter) the interaction between a charged spherical particle and a charged planar surface is usually dominated by the electrostatic interaction when the separation distance between the bodies is larger than 5–10 Å. At smaller separation distances the electrostatic forces are still important but forces such as van der Waals, solvation, and steric forces must also be considered. In this paper, the solution of the linearized Poisson–Boltzmann equation developed in the Theory section is used to calculate the electrostatic interaction energy between a sphere and a low dielectric planar surface as a function of their separation distance and under the condition of constant charge density on both surfaces. In Eq. [17] this interaction is represented as the Gibbs free energy meaning that we consider the process to take place in a system of constant pressure.

The electrostatic properties of the system are defined by the following parameters: radius of the sphere, a; surface charge density of the sphere, σ_s; charge density of the planar surface, σ_p; ionic strength of the electrolyte characterized by its inverse Debye length, κ; dielectric constant of the sphere, ϵ_s; and the temperature, T, which is kept constant to 298 K in all the calculations. In the following figures the interaction energy is plotted as a function of the distance of closest approach between the sphere and the planar surface.

The electrostatic interaction between a charged sphere and a charged low dielectric planar surface in an electrolyte solution involves several physical effects which are coupled to each other. Some of the effects are primarily dependent on the size of the sphere or its dielectric properties while others are dominated by its charge and the creation of a double layer around it, i.e., to the effect of correlation between the charged sphere and the electrolyte ions. By a suitable choice of calculation parameters for the sphere it is possible to pronounce some of the effects over others.

To begin with, the interaction energy between a small sphere with a high surface charge density and the charged planar surface is treated. In this case the interaction is dominated by the sphere net charge and the effect of changing the correlation of electrolyte ions to the planar surface and the sphere as the distance between them varies. In this system the influence of sphere size or its dielectric properties on the interaction energy is small and the results are therefore compared with the energy obtained from the Gouy–Chapman theory for a point charge interacting with a charged surface. After that follows a discussion of cases where the influence of sphere size and its dielectric properties also are of importance for the interaction energy and some comparison with results obtained by applying the Deryaguin procedure is made.

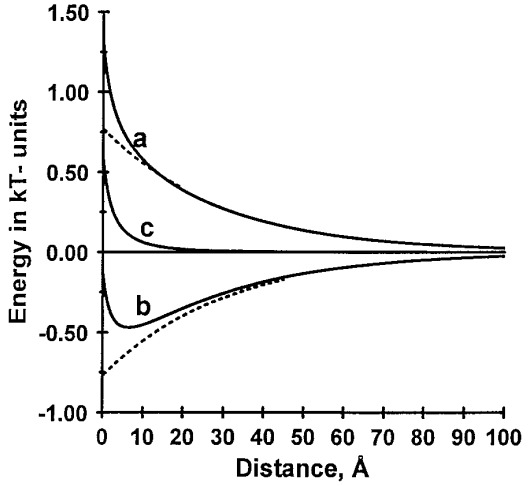

FIG. 2. Gibbs free energy as a function of separation distance between a planar surface with surface charge density 0.00472 C/m^2 and a monocharged 2.5 Å sphere: (a) $\sigma_s = 0.204$ C/m^2, (b) $\sigma_s = -0.204$ C/m^2. The dotted curves correspond to the interaction energy for a monocharged point charge calculated from the Gouy–Chapman theory. Curve (c) is the interaction energy for the monocharged 2.5 Å sphere with an uncharged surface. Debye length is 30 Å and temperature is 298 K.

In Fig. 2 the interaction energy as a function of the separation distance between a small sphere and the planar surface is shown; a comparison is also made with the interaction energy between a point charge and the charged planar surface. The curve (a) is the energy as a function of the distance between the sphere and the planar surface for a system consisting of a sphere of radius 2.5 Å carrying a unit net charge ($\sigma_s = 0.204$ C/m^2) and interacting with a similarly charged surface with $\sigma_p = 4.72 \times 10^{-3}$ C/m^2 in an electrolyte with Debye length 30 Å (= 0.01 M 1:1 salt). The upper dotted curve represents the corresponding energy for a unit point charge calculated from the Gouy–Chapman theory. Curve (b) is the energy for an oppositely monocharged 2.5 Å sphere interacting with the charged surface keeping the rest of the parameters the same as for curve (a); the lower dotted curve represents the corresponding energy for a point charge according to the Gouy–Chapman theory. Comparing curves (a) and (b) with the corresponding curves for the point charges it is clearly seen that the symmetry in the interaction is lost; i.e., the repulsion felt by the similarly charged sphere is larger than the attraction for the oppositely charged sphere. To qualitatively understand this behavior we must discuss the physical background to electrostatic interactions in an

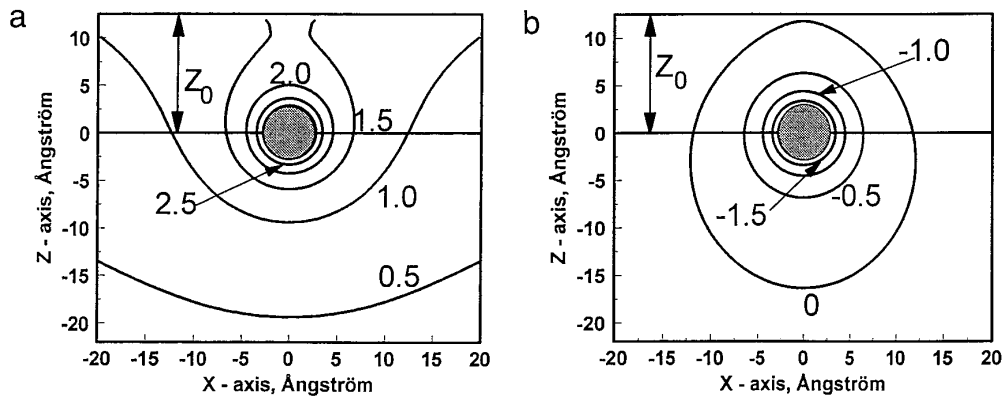

FIG. 3. Isopotential lines for a system consisting of (a) a positively monocharged and (b) a negatively monocharged ($\sigma_s = \pm 0.204$ C/m^2) 2.5 Å sphere a distance 10 Å from a planar surface with $\sigma_p = 0.00472$ C/m^2. The potential difference between the lines is 0.5 kT/e units (1 kT/e = 25.6 mV).

electrolyte system and make a comparison with the Gouy–Chapman theory.

In the Gouy–Chapman theory the pair correlation between ions within the double layer is neglected and the interaction between a point charge and a charged surface therefore becomes symmetric; i.e., ions of the same net charge but of opposite sign give equal interaction energies but of opposite sign. The major principal difference between the calculations for the small charged sphere and the point charge is the inclusion of ion correlation between the sphere and its counterions as well as the ions constituting the planar surface double layer, through the linearized Poisson–Boltzmann equation.

For the similarly charged sphere and surface, curve (a), the inclusion of ion correlation effects through the linearized P–B equation results in an overlapping of the electrostatic potential profiles of the sphere and planar surface. This in turn gives rise to two effects; (i) the creation of positive polarization charges on the low dielectric planar surface giving an image charge repulsion and (ii) an increase in electrostatic potential in the ''interacting region,'' i.e., the volume which is close to both the sphere and the planar surface, resulting in an accumulation of counterions in this region. The latter effect decreases the entropy of the electrolyte counterions and therefore contributes to the increase in the energy of the system. These effects are illustrated in Fig. 3a where isopotential curves are drawn for a separation distance, $(Z_0 - a)$, between the sphere and the surface of 10 Å; the parameters are the same as for curve(a) in Fig. 2. The electrostatic potential created close to the sphere is in this case 2.5 kT/e units which should be considered as the upper limit for the linearized Poisson–Boltzmann equation for this geometry. A numerical solution of the Poisson–Boltzmann equation and its linearized form for a sphere of this size and charge density in a 0.01 M solution gives that the potential at the sphere surface is 2.62 kT/e and 2.64 kT/e, respectively. The agreement between the two numerical values indicates that the linearized equation is approximately valid also in Fig. 3a.

When the signs of the sphere and surface charges are opposite the result of the ion correlation is more complex. The reason is that for long separation distances the overlapping of electrostatic potential profiles decreases the electrical field in the ''interacting region,'' while for short separation distances the field may increase causing an increase in system energy. This is also true for the accumulation of ions in this region; the concentration decrease for long separation distances which increases the entropy and thus decreases the system energy. As the sphere comes close to the surface the electrolyte ion concentration may increase in the interacting region giving a decrease in entropy which together with an image charge repulsion increases the system energy. This effect is illustrated by curve (b) in Fig. 2 which shows a minimum in the interaction energy vs separation distance under the same conditions as for (a) but for an oppositely charged sphere ($\sigma_s = -0.204$ C/m^2) and surface. The lowering of the potential in the interacting region, which causes the attraction to the surface, is demonstrated by comparing Fig. 3b with Fig. 3a.

A large part of the assymmetry can, to a first approximation, be accounted for by considering the energy needed to deform the sphere double layer and expel ions from it as the charged sphere approaches a low dielectric noncharged surface. This will also create an image charge repulsion since the deformation and expulsion of the sphere counterions cause an incomplete shielding of the charged sphere. Both these effects are repulsive and increase with increasing sphere charge density and with decreasing separation distance between the sphere and the surface, as is illustrated in Fig. 2 curve(c) for the monocharged 2.5 Å sphere. Almost all the difference between the calculated interaction energy for the point charge with a separation distance corresponding to the center of the sphere and the 2.5 Å sphere in Fig. 2 is explained by subtracting the function in curve(c) from (a)

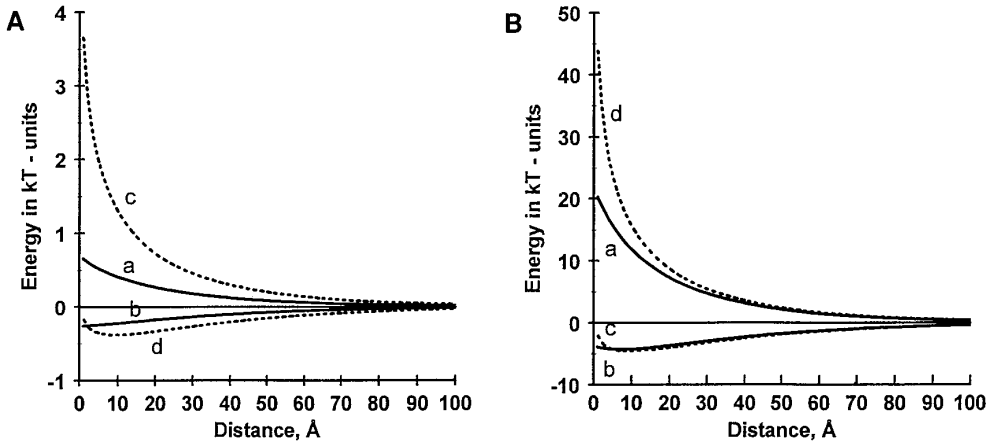

FIG. 4. (A) Gibbs free energy as a function of separation distance between a planar surface with surface charge density 0.00472 C/m^2 and a monocharged 25 Å sphere: (a) $\sigma_s = 0.00204$ C/m^2, (b) $\sigma_s = -0.00204$ C/m^2. The dotted curves (c) and (d) are the corresponding curves calculated from the Deryaguin approximation. (B) Gibbs free energy as a function of separation distance between a planar surface with surface charge density 0.00472 C/m^2 and a charged 300 Å sphere: (a) $\sigma_s = 0.00204$ C/m^2, (b) $\sigma_s = -0.00204$ C/m^2. The dotted curves (c) and (d) are the corresponding curves calculated from the Deryaguin approximation. Debye length is 30 Å, temperature is 298 K, and dielectricity constant of the sphere is 2 in both figures.

and (b), respectively, giving a curve which is very close to what is obtained for a point charge.

In the previous paragraphs the calculated interaction energy for a small monocharged sphere is compared with that for a point charge according to the Gouy–Chapman theory. For a large charged sphere interacting with a charged surface a comparison with the result from a Deryaguin-procedure approach is appropriate. A straightforward application of the Deryaguin procedure for the case of a sphere interacting with a planar surface under the condition of constant charge density on both bodies gives the following expression for the interaction energy (in kT units);

$$G_{el} = (2\pi a/\kappa\epsilon_0\epsilon_w kT) \times ((\sigma_s^2 + \sigma_p^2)((Z_0 - a) - (1/2\kappa) \times \ln(\exp(2(Z_0 - a)\kappa) - 1)) + (\sigma_s\sigma_p/\kappa) \times \ln((1 + \exp(-(Z_0 - a)\kappa))/(1 - \exp(-(Z_0 - a)\kappa)))), \quad [20]$$

where κ is the inverse Debye length, k is the Boltzmann constant, and T is the temperature; the rest of the parameters are defined in Fig. 1. A comparison between the interaction energy obtained from the Deryaguin procedure, Eq. [20], and the linearized P–B equation is done in Fig. 4a for a positively and negatively monocharged 25 Å sphere ($\sigma_s = \pm 2.04 \times 10^{-3}$ C/m^2) interacting with a planar surface with potential +20 mV ($\sigma_p = 4.72 \times 10^{-3}$ C/m^2) in an electrolyte solution characterized by the Debye length 30 Å (=0.01 M 1:1 salt solution). When the sign of the charge is the same on the two interacting surfaces the Deryaguin procedure predicts a considerably larger repulsive interaction at small separation distances than what the solution of the linearized P–B equation does. Also, for an oppositely charged sphere and surface the magnitude of the attractive interaction is larger when the Deryaguin procedure is used and another difference is that a sharp minimum occurs when the separation distance is around 10 Å. As the size of the sphere increases relative to the Debye length the relative difference between the energies obtained from the Deryaguin procedure and the corresponding P–B solution decreases. In Fig. 4b the interaction energy for a 300 Å sphere is shown keeping the rest of the parameters the same as for Fig. 4a and by comparing the two figures it is seen that for the repulsive case the relative difference has decreased from a factor of 7 to approximately 2. Also, when the sphere and surface are oppositely charged the Deryaguin procedure for the 300 Å, Fig. 4b, gives attractive energies in better agreement with the linearized P–B solution than the corresponding 25 Å sphere in Fig. 4a.

A comparison of the interaction energy for a monocharged 25 Å sphere in Fig. 4, curves (a) and (b) with that of the monocharged point charge or the monocharged 2.5 Å sphere in Fig. 2 reveals that, despite the increased repulsion from its size, the total repulsive energy has decreased. The explanation is that the charge is smeared out on a larger surface increasing the shielding effect from the electrolyte. When the sphere is negatively charged (curve (b)) the repulsive effect of its size in combination with the shielding from the electrolyte ions results in a decreased attraction when compared to both the point charge and the 2.5 Å sphere in Fig. 2.

When discussing the combined effect of sphere parameters (i.e., size, charge, and dielectricity constant) and planar surface charge density on the net interaction energy calculated from the linearized P–B equation, it is useful to make a division into three contributing components; the interaction

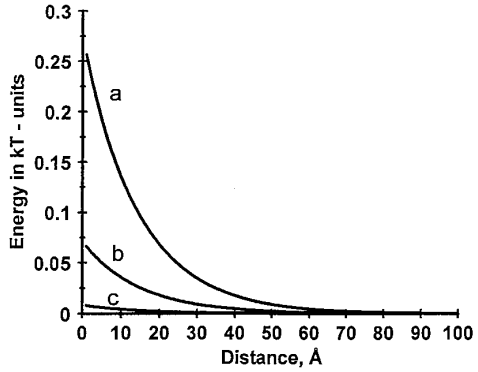

FIG. 5. Gibbs free energy as a function of separation distance between a planar surface with surface charge density 0.00472 C/m^2 and an uncharged sphere with sphere radius as a parameter: (a) a = 50 Å, (b) a = 25 Å, and (c) a = 10 Å. Debye length is 30 Å, temperature is 298 K, and dielectricity constant of sphere is 80.

between a charged planar surface and a point charge of the same net charge as the sphere situated in the center of the sphere (i.e., the Gouy–Chapman theory), the interaction between an uncharged sphere of the same size as the sphere in question and the charged planar surface, and finally the interaction between the charged sphere and an uncharged planar surface. We show later that by adding the interaction energy for these three separate components the resulting sum is a first-order approximation of the total net interaction energy for a given separation distance between the sphere and the surface. The main advantage of the division is that it is easier to qualitatively rationalize and grasp how various parameters influence the net interaction energy. In Fig. 5–8 we therefore initially discuss the interaction energy for the separate sphere and planar surface parameters and after that is illustrated how this first-order approximation compares to the more exact solution of the linearized P–B equation.

First, the interaction between uncharged spheres of different sizes and a charged planar surface is discussed. Second, the influence of the sphere dielectricity constant on the interaction is considered and thereafter the influence of planar surface charge density is shown. Finally, the interaction between spheres with different net charge interacing with an uncharged surface is illustrated.

The effect of sphere size on the interaction energy is illustrated in Fig. 5 where the interaction energy between a charged planar surface ($\sigma_p = 4.72 \times 10^{-3}$ C/m^2) with noncharged spheres with $\epsilon_s = 80$ and of different radii are shown for an electrolyte with Debye length 30 Å. When a noncharged sphere approaches the charged surface a deformation of the double layer connected to the planar surface results and a volume which is free of charges is created. The creation of a counterion free volume is a process for which the system energy increases as the size of the sphere increases and when the separation distance decreases. Furthermore, as the sphere approaches the charged planar surface there is an increase in the electrical field in the volume occupied by the sphere compared to the case when the sphere is absent, this effect also contributes to an increase in system energy. The previous assumption that the mere size of a 2.5 Å sphere has a negligible effect on the interaction energy can also be deduced from the figure.

As discussed above the electrical field created within the sphere is one of the parameters influencing the interaction energy. This parameter is in turn related to the sphere dielectric constant through the boundary condition in Eq. [15b]. The effect of the dielectric constant on the interaction energy as a function of distance is shown in Fig. 6 for a noncharged sphere with radius 25 Å. The increased repulsive interaction energy when decreasing the dielectric constant is due to the increased electrical field in the low dielectric sphere and to the loss of entropy because of the increased concentration of counterions in the ''interacting region.'' When the dielectric constant is sufficiently high, illustrated in the figure with $\epsilon_s = 500$, the decrease in electrical field within the sphere compared to the fields in the double layer in absence of the sphere, more than compensates for the creation of a charged free volume leading to a decrease in system energy.

Since both the concentration of counterions in the double layer as well as the electrical field increase with increasing planar surface charge density, the previous discussion suggests that the charge density of the planar surface is a parameter influencing the interaction between an uncharged sphere and a charged sphere. This is illustrated in Fig. 7 for the interaction between a 25 Å sphere ($\epsilon_s = 80$) and planar surfaces with different surface charge densities for a constant Debye length of 30 Å. The curves in Fig. 7 show that the repulsion of a given sphere increases when the surface charge density on the planar surface increases.

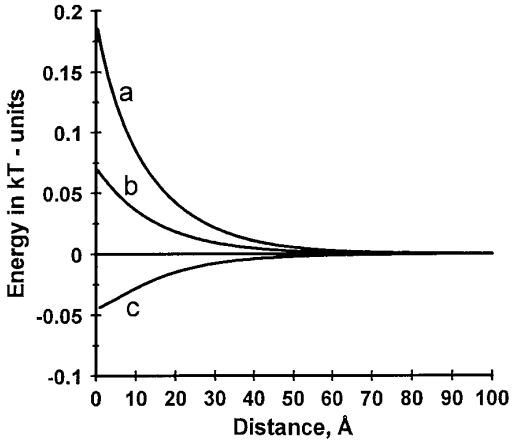

FIG. 6. Gibbs free energy as a function of separation distance between a planar surface with surface charge density 0.00472 C/m^2 and an uncharged 25 Å sphere with sphere dielectricity constant as a parameter: (a) $\epsilon_s = 2$, (b) $\epsilon_s = 80$, and (c) $\epsilon_s = 500$. Debye length is 30 Å and temperature is 298 K.

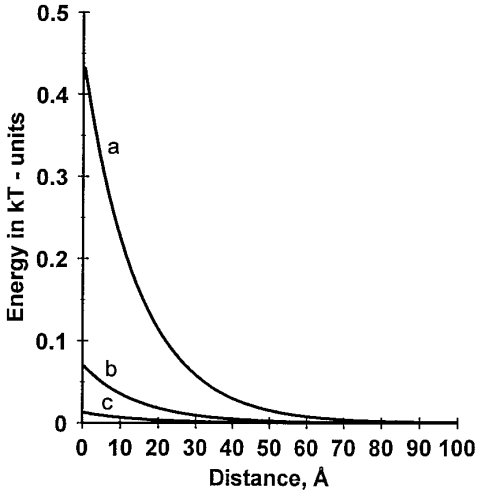

FIG. 7. Gibbs free energy as a function of separation distance between an uncharged 25 Å sphere and a planar surface with planar surface charge density as a parameter: (a) $\sigma_p = 0.0118$ C/m^2, (b) $\sigma_p = 0.00472$ C/m^2, and (c) $\sigma_p = 0.00204$ C/m^2. Debye length is 30 Å, temperature is 298 K, and sphere dielectricity constant is 80.

A system consisting of a charged sphere and an uncharged planar surface is analogous to the previously discussed charged surface and an uncharged sphere, a repulsive interaction is therefore expected. Examples are shown in Fig. 8 where the charge densities of the 25 Å sphere are chosen to the same numerical values as the planar surface in Fig. 7, the rest of the parameters the same in the two figures. Comparing the results in the two figures reveals that the repulsive interaction energy is larger when the sphere is charged than when the planar surface is.

In the following figures some examples of the interaction energy calculated from the linearized P–B equation are

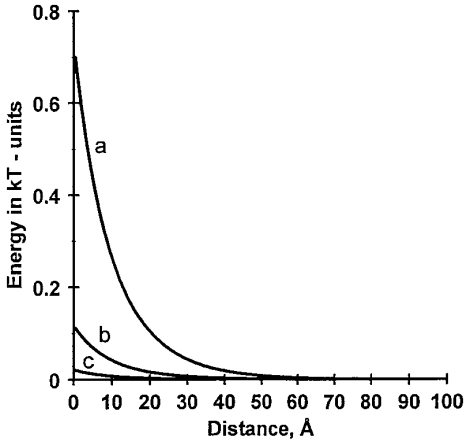

FIG. 8. Gibbs free energy as a function of separation distance between a planar surface and a charged 25 Å sphere with surface charge density as a parameter: (a) $\sigma_s = 0.0118$ C/m^2 ($q = 5.78$), (b) $\sigma_s = 0.00472$ C/m^2 ($q = 2.31$), and (c) $\sigma_s = 0.00204$ C/m^2 (sphere charge $q = 1$). Debye length is 30 Å, temperature is 298 K, and sphere dielectricity constant is 80.

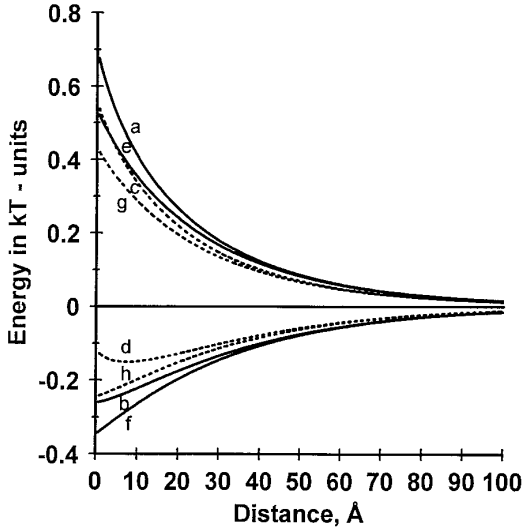

FIG. 9. Gibbs free energy as a function of separation distance between a charged planar surface ($\sigma_p = 0.00472$ C/m^2) and a monocharged 25 Å sphere ($\sigma_s = \pm 0.00204$ C/m^2). The full lines are calculated from the numerical solution of the linearized P–B equation, while the dotted lines are obtained from the summation discussed in the text. (a) $\sigma_s = 0.00204$ C/m^2, $\epsilon_s = 2$; (b) $\sigma_s = -0.00204$ C/m^2, $\epsilon_s = 2$; (c) parameters as in (a); (d) parameters as in (b); (e) $\sigma_s = 0.00204$ C/m^2, $\epsilon_s = 80$; (f) $\sigma_s = -0.00204$ C/m^2, $\epsilon_s = 80$; (g) parameters as in (e); (h) parameters as in (f). Debye length is 30 Å and temperature is 298 K.

shown and the meanings of respective curves are: (a) The interaction energy between a similarly and (b) oppositely monocharged sphere ($\epsilon_s = 2$) and surface. Curves(e) and (f) represent the interaction energy between a similarly and oppositely monocharged sphere and planar surface with $\epsilon_s = 80$, respectively. The difference between this interaction energy and the energy in curves(a) and (b) is due to the lower dielectricity constant of the sphere. In these figures the dotted curves (c), (d), (g), and (h) correspond to the interaction energy obtained by adding the contributions from the separate components; monocharged point charge interacting with the charged surface and located in the center of the sphere plus the interaction energy between an uncharged 25 Å sphere and the charged surface plus the interaction energy between the monocharged 25 Å sphere and the uncharged surface.

The full lines in Fig. 9 show the interaction energy as function of separation distance obtained from the solution of the linearized P–B equation for a positively and negatively monocharged 25 Å sphere with $\epsilon_s = 2$ and 80, respectively, interacting with a positively charged planar surface in an electrolyte with Debye length 30 Å. When the sphere and the surface both are positively charged the repulsion is stronger for the low dielectric sphere and when they carry opposite charge its attractive interaction energy is smaller. The dotted curves corresponding to each full curve represent the interaction energy obtained from addition of the components as is discussed in the previous paragraph. A qualitative

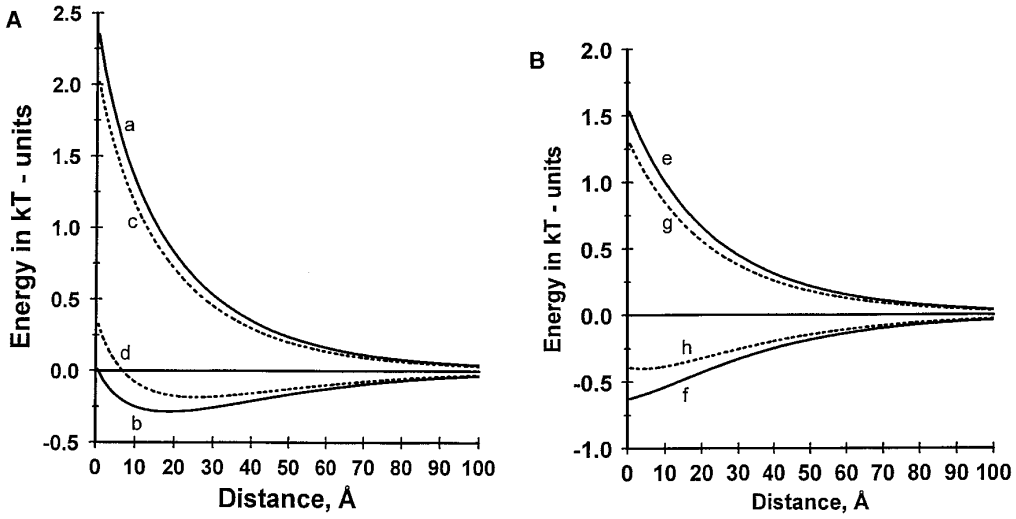

FIG. 10. (A) Gibbs free energy as a function of separation distance between a charged planar surface ($\sigma_p = 0.0118$ C/m^2) and a monocharged 25 Å sphere ($\sigma_s = \pm 0.00204$ C/m^2). The full lines are calculated from the numerical solution of the linearized P–B equation while the dotted lines are obtained from the summation discussed in the text. (a) $\sigma_s = 0.00204$ C/m^2, $\epsilon_s = 2$; (b) $\sigma_s = -0.00204$ C/m^2, $\epsilon_s = 2$; (c) parameters as in (a); (d) parameters as in (b). (B) (e) $\sigma_s = 0.00204$ C/m^2, $\epsilon_s = 80$; (f) $\sigma_s = -0.00204$ C/m^2, $\epsilon_s = 80$; (g) parameters as in (e); (h) parameters as in (f). Debye length is 30 Å and temperature is 298 K in both figures.

agreement between the two sets of curves is obtained with some deviation occurring at short separation distances. Comparison with Figs. 5 and 6 reveals that the major contribution to the assymmetry in interaction between the oppositely charged spheres can be rationalized as the repulsion due to the penetration of the uncharged sphere into the planar surface double layer.

In Figs. 10a and 10b the parameters are the same as for Fig. 9 except that the charge density of the planar surface has increased to 11.8×10^{-3} C/m^2. A comparison of the two figures shows that the increase of planar charge density increases the repulsive interaction between similarly charged bodies. It is interesting to note that although the planar surface charge density increased, the attractive interaction decreased for the oppositely charged low dielectric sphere. To a first approximation these results are rationalized through the addition of the previously proposed separate components, which are represented by the corresponding dotted curves in the figures. Comparison with Fig. 7 shows that the component that contributes most to the strong assymmetry in the interaction is the deformation of the planar surface double layer caused by the penetration of the sphere, an interaction which strongly depends on the dielectricity constant of the sphere.

The role of an increased sphere net charge on the interaction with a charge planar surface is illustrated in Fig. 11 where the numerical value of the sphere charge has increased to ± 5.78 ($\sigma_s = \pm 11.78 \times 10^{-3}$ C/m^2), keeping the value of the rest of the parameters the same as for Fig. 9. Comparison with Fig. 9 shows that the increase in sphere net charge results in an almost proportional increase in both repulsive and attractive interaction and that the effect of the sphere dielectricity constant is small. The dotted curves, representing the added components, are for all cases close to the real curves and a comparison with Figs. 7 and 8 shows that the component giving the assymmetric interaction is primarily the deformation of the double layer coupled to the sphere.

SUMMARY AND CONCLUSION

In summary, the increase in system energy when a charged sphere approaches a similarly charged planar surface is

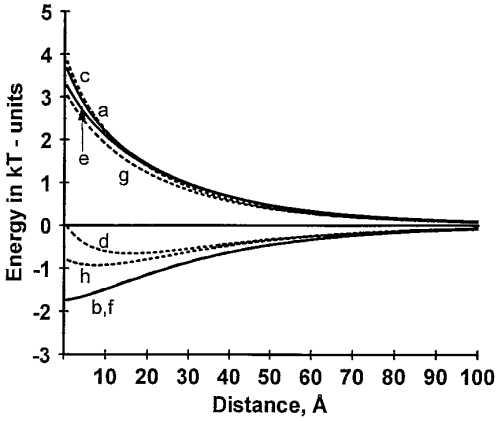

FIG. 11. Gibbs free energy as a function of separation distance between a charged planar surface ($\sigma_s = 0.00472$ C/m^2) and a charged 25 Å sphere ($\sigma_p = \pm 0.0118$ C/m^2, i.e., sphere net charge is 5.78). The full lines are calculated from the numerical solution of the linearized P–B equation while the dotted lines are obtained from the summation discussed in the text. (a) $\sigma_s = 0.0118$ C/m^2, $\epsilon_s = 2$; (b) $\sigma_s = -0.0118$ C/m^2, $\epsilon_s = 2$; (c) parameters as in (a); (d) parameters as in (b); (e) $\sigma_s = 0.0118$ C/m^2, $\epsilon_s = 80$; (f) $\sigma_s = -0.0118$ C/m^2, $\epsilon_s = 80$; (g) parameters as in (e); (h) parameters as in (f). Debye length is 30 Å and temperature is 298 K.

caused by an interaction between the charges on the two bodies, the creation of an electrical field within the sphere, and an accumulation of ions in the volume between the two bodies, the ''interacting region.'' The decrease in system energy that occurs when an oppositely charged surface and sphere interact is also due to the interaction between the charges on the two bodies but in this case there is a decrease of the electrostatic potential in the ''interacting region'' and a corresponding release of ions from this region giving an increase in entropy. This effect is always operating at long separation distances. For short separation distances and when there is a large difference between the charge density of the sphere and the surface, the electrostatic potential increases and the electrolyte ions accumulate in the ''interacting region'' as the separation distance decreases. Another effect which also gives a contribution to the increase in system energy when the separation distance decreases is the energy needed to expel the ions in the double layer from the volume occupied by the sphere formation and the corresponding creation of an electrical field within the sphere. The latter effect is also operative when the sphere or planar surface, respectively, are uncharged giving a net repulsion which increase when the separation distance decreases.

Because the electrolyte ions respond to changes in the electrostatic potential the previously discussed effects are all closely connected to each other and are generally not additive. The general thermodynamic criterion for the system is to minimize the free energy at a given separation distance which is a balance between the energy created by the electrical field and the loss of entropy which accompanies the accumulation of counterions into regions of high electrostatic potentials. It is, however, difficult to visualize how the different parameters influence this balance. In order to more easily gain physical insight a semiquantitative approach is suggested and compared with the exact solution of the linearized P–B equation developed in the paper. The approximative view consists of three separate components: the interaction between the charged planar surface and a point charge with the same net charge as the sphere and located in the center of the sphere, the interaction energy between the uncharged sphere and the charged surface, and the interaction energy between the charged sphere and the uncharged surface.

REFERENCES

1. Ståhlberg, J., Jönsson, B., Horvath, Cs., *Anal. Chem.* **63,** 1867 (1991).
2. Debye, P., and Huckel, E., *Phys. Z.* **24,** 185 (1923).
3. Dube, G. P., *Ind. J. Phys.* **17,** 189 (1943).
4. Deryaguin, B., *Trans. Faraday Soc.* **36,** 203 (1940).
5. Verwey, E. J. W., and Overbeek, J. Th. G., ''Theory of the Stability of Lyophobic Colloids.'' Elsevier, Amsterdam, 1948.
6. Medina-Noyola, M., and McQuarrie, D. A., *J. Chem. Phys.* **73,** 6279 (1980).
7. Hogg, R., Healy, T. W., and Furstenau, D. W., *Trans. Faraday Soc.* **62,** 1638 (1966).
8. McCartney, L. N., and Levine, S., *J. Colloid Interface Sci.* **30,** 345 (1969).
9. Honig, E. P., and Mul, P. M., *J. Colloid Interface Sci.* **36,** 258 (1971).
10. Bentz, J., *J. Colloid Interface Sci.* **90,** 164 (1982).
11. Ring, T. J., *Chem. Soc. Faraday Trans.* **78,** 1513 (1982).
12. Krozel, J. W., and Saville, D. A., *J. Colloid Interface Sci.* **150,** 365 (1992).
13. Overbeek, J. Th. G., *J. Chem. Soc. Faraday Trans.* **84,** 3079 (1988).
14. Kaplan, F. S., Solomak, T. B., and Brosov, K. N., *Kolloid. Zh.* **51,** 867 (1989).
15. Kaplan, F. S., Solomak, T. B., and Brosov, K. N., *Kolloid. Zh.* **51,** 1100 (1989).
16. Carnie, S. L., Chan, D. Y. C., and Gunning, J. S., *Langmuir* **10,** 2993 (1994).
17. Ohshima, H., and Kondo, T., *J. Colloid Interface Sci.* **157,** 504 (1993).
18. Jackson, J. D., ''Classical Electrodynamics.'' Wiley, New York, 1962.
19. Hiemenz, P. G., ''Principles of Colloid and Surface Chemistry.'' Dekker, New York, 1986.
20. Arfken, G., ''Mathematical Methods for Physicists.'' Academic Press, New York, 1968.
21. Abramovitz, M., and Stegun, I. A., ''Handbook of Mathematical Functions.'' Dover, New York, 1970.
22. Jönsson, B., and Wennerström, H., *Chem. Scr.* **22,** 221 (1983).